


Impurity-Induced Smearing of the Spin Resonance Peak in Fe-Based Superconductors

Yu. N. Togushova¹ · V. A. Shestakov¹ ·
M. M. Korshunov^{1,2} 

Received: 14 July 2015 / Accepted: 2 March 2016 / Published online: 14 March 2016
© Springer Science+Business Media New York 2016

Abstract The spin resonance peak in the iron-based superconductors is observed in inelastic neutron scattering experiments and agrees well with predicted results for the extended s -wave (s_{\pm}) gap symmetry. On the basis of four-band and three-orbital tight-binding models we study the effect of nonmagnetic disorder on the resonance peak. Spin susceptibility is calculated in the random-phase approximation with the renormalization of the quasiparticle self-energy due to the impurity scattering in the static Born approximation. We find that the spin resonance becomes broader with the increase of disorder and its energy shifts to higher frequencies. For the same amount of disorder the spin response in the s_{\pm} state is still distinct from that of the s_{++} state.

Keywords Fe-based superconductors · Spin resonance peak · Spin–orbit coupling · Impurity scattering

1 Introduction

The discovery of Fe-based superconductors (FeBS) in 2008 with a maximal T_c of 55 K gave rise to the debates on the origin of the superconducting state. FeBS can be broadly divided into two classes, pnictides and chalcogenides [1–3]. Since conductivity is provided by the FeAs layer, the discussion of physics in terms of quasi two-dimensional system in most cases gives reasonable results [4]. Fe d -orbitals form the Fermi surface (FS) that excludes the cases of extreme hole and electron dopings consisting of two hole sheets around the $\Gamma = (0, 0)$ point and two electron sheets around the $M = (\pi, \pi)$

✉ M. M. Korshunov
mkor@iph.krasn.ru

¹ Siberian Federal University, Svobodny Prospect 79, Krasnoyarsk, Russia 660041

² L.V. Kirensky Institute of Physics, Krasnoyarsk, Russia 660036

point in the 2-Fe Brillouin zone (BZ). In the 1-Fe BZ, the latter corresponds to the electron sheets around the $(\pi, 0)$ and $(0, \pi)$ points. Nesting between these two groups of sheets is the driving force for the spin-density wave (SDW) long-range magnetism in the undoped FeBS. Upon doping the SDW state is destroyed, but the residual scattering with the wave vector \mathbf{Q} connecting hole and electron pockets naturally leads to enhanced antiferromagnetic fluctuations. \mathbf{Q} is equal to (π, π) in the 2-Fe BZ and to $(\pi, 0)$ or $(0, \pi)$ in the 1-Fe BZ.

Different mechanisms of Cooper pair formation result in distinct superconducting gap symmetry and structure [4]. In particular, the RPA-SF (random-phase approximation spin fluctuation) approach gives the extended s -wave gap that changes sign between hole and electron Fermi surface sheets (s_{\pm} state) as the main instability for a wide range of doping concentrations [4–6]. On the other hand, orbital fluctuations promote the order parameter to have the sign-preserving s_{++} symmetry [7]. Thus, probing the gap structure can help in elucidating the underlying mechanism. In this respect, inelastic neutron scattering is a powerful tool since the measured dynamical spin susceptibility $\chi(\mathbf{q}, \omega)$ in the superconducting state carries information about the gap structure.

For the local interactions (Hubbard and Hund's exchange), χ can be obtained in the RPA from the bare electron–hole bubble $\chi_0(\mathbf{q}, \omega)$ by summing up a series of ladder diagrams to give

$$\chi(\mathbf{q}, \omega) = I - U_s \chi_0(\mathbf{q}, \omega)^{-1} \chi_0(\mathbf{q}, \omega), \quad (1)$$

where U_s and I are interaction and unit matrices in orbital or band space, and all other quantities are matrices as well. Scattering between nearly nested hole and electron Fermi surfaces in FeBS produce a peak in the normal-state magnetic susceptibility at or near $\mathbf{q} = \mathbf{Q}$. For the uniform s -wave gap, $\text{sign}\Delta_{\mathbf{k}} = \text{sign}\Delta_{\mathbf{k}+\mathbf{Q}}$ and there is no resonance peak. For the s_{\pm} order parameter as well as for an extended non-uniform s -wave symmetry, \mathbf{Q} connects Fermi sheets with the different signs of gaps. This fulfills the resonance condition for the interband susceptibility, and the spin resonance peak is formed at a frequency ω_s below $\Omega_c = \min |\Delta_{\mathbf{k}}| + |\Delta_{\mathbf{k}+\mathbf{q}}|$. The existence of the spin resonance in FeBS was predicted theoretically [8,9] and subsequently discovered experimentally with many reports of well-defined spin resonances in all systems, see [4].

Since there is always some amount of disorder even in the crystals of a very good quality, it is necessary to study the evolution of the spin response with increasing amount of disorder. Here we do this within two models for the band structure—one is the simple four-band model in the 2-Fe BZ [8] and the other one is the three-orbital model in the 1-Fe BZ [10] with the spin–orbit coupling [11]. The effect of disorder on the spin susceptibility is incorporated via the static Born approximation for the quasiparticle self-energy due to the impurity scattering.

2 Models and Approximations

We study the spin response in the superconducting state of FeBS within the tight-binding models for the two-dimensional iron layer. Some basic information can be

gained from the four-band model of Ref. [8], that is able to reproduce the FS obtained via band structure calculations. It has the following single-electron Hamiltonian $H_0 = \sum_{\mathbf{k}, \alpha, \sigma} \varepsilon^i n_{\mathbf{k}i\sigma} - \sum_{\mathbf{k}, i, \sigma} t_{\mathbf{k}}^i d_{\mathbf{k}i\sigma}^\dagger d_{\mathbf{k}i\sigma}$, where $d_{\mathbf{k}i\sigma}$ is the annihilation operator of the d -electron with momentum \mathbf{k} , spin σ , and band index $i = \{\alpha_1, \alpha_2, \beta_1, \beta_2\}$, ε^i are the on-site single-electron energies, $t_{\mathbf{k}}^{\alpha_1, \alpha_2} = t_1^{\alpha_1, \alpha_2} \cos k_x + \cos k_y + t_2^{\alpha_1, \alpha_2} \cos k_x \cos k_y$ is the electronic dispersion that yields hole pockets centered around the Γ point, and $t_{\mathbf{k}}^{\beta_1, \beta_2} = t_1^{\beta_1, \beta_2} \cos k_x + \cos k_y + t_2^{\beta_1, \beta_2} \cos \frac{k_x}{2} \cos \frac{k_y}{2}$ is the dispersion that results in the electron pockets around the M point. Using the abbreviation $(\varepsilon^i, t_1^i, t_2^i)$ we choose the parameters $(-0.60, 0.30, 0.24)$ and $(-0.40, 0.20, 0.24)$ for the α_1 and α_2 bands, respectively, and $(1.70, 1.14, 0.74)$ and $(1.70, 1.14, -0.64)$ for the β_1 and β_2 bands, correspondingly (all values are in eV).

The matrix elements of the bare spin susceptibility in the multiband system has the form: $\chi_0^{ij}(\mathbf{q}, i\Omega) = -\frac{T}{2} \sum_{\mathbf{k}, \omega_n} G^i(\mathbf{k} + \mathbf{q}, i\omega_n + i\Omega) G^j(\mathbf{k}, i\omega_n) + F^i(\mathbf{k} + \mathbf{q}, i\omega_n + i\Omega) F^j(\mathbf{k}, i\omega_n)$, where Ω and ω_n are Matsubara frequencies, G^i and F^i are the normal and anomalous (superconducting) Green's functions, respectively. Physical spin susceptibility $\chi(\mathbf{q}, i\Omega) = \sum_{i,j} \chi^{i,j}(\mathbf{q}, i\Omega)$ obtained by calculating matrix elements $\chi^{i,j}(\mathbf{q}, i\Omega)$ via equation (1) with the interaction matrix $U_s^{i,j} = \tilde{U} \delta_{i,j} + \tilde{J}/2(1 - \delta_{i,j})$. We assume here the effective Hubbard interaction parameters to be $\tilde{J} = 0.2\tilde{U}$ and $\tilde{U} \sim t_1^{\beta_1}$ in order to stay in the paramagnetic phase [8]. We consider the magnetic susceptibility in the superconducting state assuming the s_{\pm} state with $\Delta_{\mathbf{k}} = \frac{\Delta_0}{2} \cos k_x + \cos k_y$, where Δ_0 was chosen to be 5 meV.

The model described above lack for the orbital content of the bands. Now we introduce an additional level of complexity by considering the three-orbital model in the 1-Fe BZ [10]. By introducing the spin-orbit (SO) interaction to it [11], it is possible to explain the observed anisotropy of the spin resonance peak in Ni-doped Ba-122 [12]. In particular, χ_{+-} and $2\chi_{zz}$ components of the spin susceptibility are different thus breaking the spin-rotational invariance $\langle S_+ S_- \rangle = 2 \langle S_z S_z \rangle$. This model comes from the three t_{2g} d -orbitals. The xz and yz components are hybridized and form two electron-like FS pockets around $(\pi, 0)$ and $(0, \pi)$ points, and one hole-like pocket around $\Gamma = (0, 0)$ point. The xy orbital is considered to be decoupled from them and form an outer hole pocket around Γ point. The latter differs from some popular orbital models for FeBS [4, 5]. However, according to ARPES data [13, 14] and the DFT calculations for highly doped systems [15] and undoped 122, 1111, and 111 materials [16–18], xy orbital contribution to the Fermi surface near Γ point is quite large in the 2-Fe Brillouin zone. This situation is simulated by introducing the xy hole pocket near Γ point in the three-orbital model. The Hamiltonian is given by $H = H_0 + H_{SO}$, where $H_0 = \sum_{\mathbf{k}, \sigma, l, m} \varepsilon_{\mathbf{k}}^{lm} c_{\mathbf{k}l\sigma}^\dagger c_{\mathbf{k}m\sigma}$ is one-electron part with $c_{\mathbf{k}m\sigma}$ being the annihilation operator of a particle with momentum \mathbf{k} , spin σ , and orbital index m . Keeping in mind the similarity of H_0 to the Sr_2RuO_4 case, for simplicity we consider only the L_z -component of the SO interaction, which affects xz and yz bands only [19]. The matrix

$$\text{of the full Hamiltonian } H \text{ has the form } \hat{\varepsilon}_{\mathbf{k}\sigma} = \begin{pmatrix} \varepsilon_{1\mathbf{k}} & 0 & 0 \\ 0 & \varepsilon_{2\mathbf{k}} & \varepsilon_{4\mathbf{k}} + i\frac{\lambda}{2} \text{sign}\sigma \\ 0 & \varepsilon_{4\mathbf{k}} - i\frac{\lambda}{2} \text{sign}\sigma & \varepsilon_{3\mathbf{k}} \end{pmatrix},$$

where $\varepsilon_{1\mathbf{k}} = \varepsilon_{xy} - \mu + 2t_{xy}(\cos k_x + \cos k_y) + 4t'_{xy} \cos k_x \cos k_y$, $\varepsilon_{2\mathbf{k}} = \varepsilon_{yz} - \mu + 2t_x \cos k_x + 2t_y \cos k_y + 4t'' \cos k_x \cos k_y + 2t'''(\cos 2k_x + \cos 2k_y)$, $\varepsilon_{3\mathbf{k}} = \varepsilon_{xz} - \mu + 2t_y \cos k_x + 2t_x \cos k_y + 4t' \cos k_x \cos k_y + 2t''(\cos 2k_x + \cos 2k_y)$, $\varepsilon_{4\mathbf{k}} = 4t_{xyz} \sin k_x/2 \sin k_y/2$. To reproduce the topology of the FS in pnictides, we choose the following parameters (in eV): $\mu = 0$, $\varepsilon_{xy} = -0.70$, $\varepsilon_{yz} = -0.34$, $\varepsilon_{xz} = -0.34$, $t_{xy} = 0.18$, $t'_{xy} = 0.06$, $t_x = 0.26$, $t_y = -0.22$, $t' = 0.2$, $t'' = -0.07$, $t_{xyz} = 0.38$. As in the case of Sr_2RuO_4 , eigenvalues of $\hat{\varepsilon}_{\mathbf{k}\sigma}$ do not depend on the spin σ , therefore, spin-up and spin-down states are still degenerate in spite of the SO interaction.

The components of the physical spin susceptibility $\chi_{+-,zz}(\mathbf{q}, i\Omega) = \frac{1}{2} \sum_{l,m} \chi_{+-,zz}^{ll,mm}(\mathbf{q}, i\Omega)$ are calculated using Eq. (1) with the interaction matrix U_s from Ref. [5]. We choose the following values for the interaction parameters: spin–orbit coupling constant $\lambda = 100$ meV, intraorbital Hubbard $U = 0.9$ eV, Hund's $J = 0.1$ eV, interorbital $U' = U - 2J$, and pair-hopping term $J' = J$. In the superconducting state we assume either the s_{++} state with $\Delta_{\mathbf{k}} = \Delta_0$ or the s_{\pm} state with $\Delta_{\mathbf{k}} = \Delta_0 \cos k_x \cos k_y$, where $\Delta_0 = 20$ meV.

As was shown recently [20–22], the multiband superconductors may demonstrate behavior much more complicated than originally expected from the Abrikosov–Gor'kov theory [23]. In particular, $s_{\pm} \rightarrow s_{++}$ transition may take place for the sizeable intraband attraction in the two-band s_{\pm} model with the nonmagnetic impurities [20]. Discussion of such effects is well beyond the scope of the present study since it requires a self-consistent solution of the frequency and gap equations within the strong-coupling T -matrix approximation. Here we use a simple static Born approximation for the quasiparticle self-energy to see the basic effects of nonmagnetic disorder on the spin resonance. That is, the multiple scattering on the same impurity results in the following self-energy: $\Sigma(\mathbf{k}) \approx -\frac{i}{2\tau_{\mathbf{k}}}$ with $\tau_{\mathbf{k}}$ being the quasiparticle lifetime (see, e.g., the so-called first Born approximation in Ref. [24]). Calculating the exact momentum dependence of the quasiparticle lifetime is again the separate complicated task that would require realistic multiorbital models with a proper orbital-to-band contribution similar to what was done for the calculation of the transport coefficients in Ref. [25]. This is again beyond the scope of the present work, so, neglecting the momentum dependence of $\tau_{\mathbf{k}}$, we set $\Sigma(\mathbf{k}, i\Omega) = -i\Gamma$, where we treat the impurity scattering rate Γ as a parameter.

3 Results and Discussion

First, we consider the spin response in the four-band model. The result of the analytical continuation ($i\Omega_n \rightarrow \Omega + i\delta$ with $\delta \rightarrow 0+$) is shown in Fig. 1 for the set of impurity scattering rates Γ . In the case of small Γ , the spin resonance peak is clearly seen below the energy of $2\Delta_0$. With increasing Γ it becomes broader and almost vanishes once Γ becomes comparable to Δ_0 . We can trace the energy of the spin resonance ω_s as a function of Γ . Value of ω_s is determined as the maximum of $\text{Im}\chi(\mathbf{Q}, \Omega)$. The result is shown in Fig. 1. Clearly, ω_s shifts to higher frequencies with increasing disorder.

These findings are in good agreement with the results of Ref. [26] where the band model was simpler than used here, but the vertex corrections in the particle–hole bubble due to the impurity scattering were included. In particular, for the same reduction of

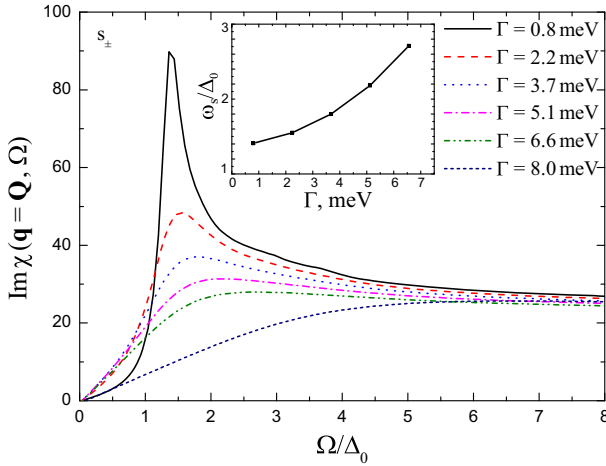


Fig. 1 Calculated $\text{Im}\chi(\mathbf{Q}, \Omega)$ with $\mathbf{Q} = (\pi, \pi)$ in the 2-Fe BZ for the four-band model in the s_{\pm} state (main panel) and the spin resonance frequency ω_s determined as the maximum of $\text{Im}\chi(\mathbf{Q}, \Omega)$ (inset) for different values of the impurity scattering rate Γ . The spin resonance below $\Omega = 2\Delta_0$ becomes much broader with increasing Γ and effectively disappears for $\Gamma > \Delta_0$ (Color figure online)

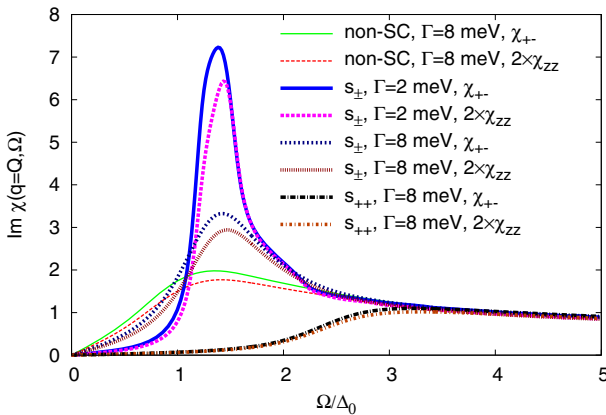


Fig. 2 Calculated $\text{Im}\chi(\mathbf{Q}, \Omega)$ with $\mathbf{Q} = (\pi, 0)$ in the 1-Fe BZ in the normal state, and for the s_{++} and s_{\pm} pairing symmetries. In the latter case, the resonance is clearly seen below $\Omega = 2\Delta_0$ (Color figure online)

the resonance peak height we see a similar broadening of the peak and small changes in the resonance frequency. Such agreement implies that the vertex corrections do not play a crucial role in the low-energy spin response while they are known to be important for the proper calculation of the transport coefficients. On the other hand, compared to Ref. [26], we go to larger values of the scattering rate and observe a nonlinear increase of the resonance frequency.

Now we switch to the three-orbital model. We calculated both $+-$ and zz components of the spin susceptibility and confirmed that in the non-superconducting state $\chi_{+-} > 2\chi_{zz}$ at small frequencies, see Fig. 2. For the s_{\pm} superconductor we observe a

well-defined spin resonance and χ_{+-} is again larger than $2\chi_{zz}$ [11]. Interestingly, for the s_{++} state the disparity between χ_{+-} and $2\chi_{zz}$ is extremely small. With increasing impurity scattering rate the spin resonance peak broadens and its energy shifts to higher frequencies. This is similar to the results in the four-band model so we conclude that the orbital character and the SO coupling do not have much effect on the impurity-induced smearing of the spin resonance within the present approximation for the quasiparticle self-energy. Note that the spin response in the s_{\pm} state is still distinct from the one in the s_{++} state even for a sizeable value of Γ . This is important for the discussion of inelastic neutron data. Since all real materials are prone to disorder the natural question arises: is it possible to distinguish between s_{\pm} and s_{++} states in the presence of nonmagnetic impurities looking at the neutron data? Here we demonstrate that if the answer is yes, then spin responses would be quite different. And the other important difference comes from the negligible disparity of χ_{+-} and $2\chi_{zz}$ components in the s_{++} state, that contradicts the results of the polarized neutron data [12].

4 Conclusion

We analyzed the spin response in the superconducting state of FeBS in the presence of nonmagnetic disorder. The disorder was treated in the simple static Born approximation thus giving only basic qualitative trends. The average impurity scattering rate Γ was considered as a parameter. For the small Γ , the spin resonance peak is clearly observed below the energy of $2\Delta_0$ and with increasing Γ it becomes broader and almost vanishes once Γ becomes comparable to Δ_0 . The energy of the spin resonance ω_s (determined as the maximum of the spin susceptibility) shifts to higher frequencies with increasing disorder. The spin resonance peak gains anisotropy in spin space due to the spin–orbit coupling, so for the s_{\pm} superconductor χ_{+-} is larger than $2\chi_{zz}$. On the other hand, for the s_{++} state the disparity between transverse and longitudinal components is negligible. The spin response in the s_{\pm} state is still distinct from that in the s_{++} state even for a sizeable value of Γ .

Acknowledgments We acknowledge partial support by the RFBR (Grant 13-02-01395), President Grant for Government Support of the Leading Scientific Schools of the Russian Federation (NSh-2886.2014.2), and The Ministry of education and science of Russia (GF-2, SFU).

References

1. M.V. Sadovskii, *Physics-Uspekhi* **51**, 1201 (2008)
2. D.C. Johnston, *Adv. Phys.* **59**, 803 (2010)
3. G.R. Stewart, *Rev. Mod. Phys.* **83**, 1589 (2011)
4. P.J. Hirschfeld, M.M. Korshunov, I.I. Mazin, *Rep. Prog. Phys.* **74**, 124508 (2011)
5. S. Graser, T.A. Maier, P.J. Hirschfeld, D.J. Scalapino, *New. J. Phys.* **11**, 025016 (2009)
6. M.M. Korshunov, *Physics-Uspekhi* **57**, 813 (2014)
7. H. Kontani, S. Onari, *Phys. Rev. Lett.* **104**, 157001 (2010)
8. M.M. Korshunov, I. Eremin, *Phys. Rev. B* **78**, 140509(R) (2008)
9. T.A. Maier, D.J. Scalapino, *Phys. Rev. B* **78**, 020514(R) (2008)
10. M.M. Korshunov, Y.N. Togushova, I. Eremin, *J. Supercond. Nov. Magn.* **26**, 2665 (2013)
11. M.M. Korshunov, Y.N. Togushova, I. Eremin, P.J. Hirschfeld, *J. Supercond. Nov. Magn.* **26**, 2873 (2013)

12. O.J. Lipscombe et al., Phys. Rev. B **82**, 064515 (2010)
13. V. Brouet, M.F. Jensen, P.-H. Lin, A. Taleb-Ibrahimi, P. Le Fevre, F. Bertran, C.-H. Lin, W. Ku, A. Forget, D. Colson, Phys. Rev. B **86**, 075123 (2012)
14. A.A. Kordyuk, Low Temp. Phys. **38**, 1119 (2012)
15. S. Backes, D. Guterding, H.O. Jeschke, R. Valenti, New J. Phys. **16**, 083025 (2014)
16. I.A. Nekrasov, private communications
17. I.A. Nekrasov, Z.V. Pchelkina, M.V. Sadovskii, JETP Lett. **88**, 144 (2008)
18. I.A. Nekrasov, Z.V. Pchelkina, M.V. Sadovskii, JETP Lett. **88**, 543 (2008)
19. I. Eremin, D. Manske, K.H. Bennemann, Phys. Rev. B **65**, 220502(R) (2002)
20. D.V. Efremov, M.M. Korshunov, O.V. Dolgov, A.A. Golubov, P.J. Hirschfeld, Phys. Rev. B **84**, 180512(R) (2011)
21. V.G. Stanev, A.E. Koshelev, Phys. Rev. B **86**, 174515 (2012)
22. M.M. Korshunov, D.V. Efremov, A.A. Golubov, O.V. Dolgov, Phys. Rev. B **90**, 134517 (2014)
23. A.A. Abrikosov, L.P. Gor'kov, Sov. Phys. JETP **12**, 1243 (1961) [J. Exptl. Theoret. Phys. (U.S.S.R.) **39**, 1781 (1960)]
24. H. Bruus, K. Flensberg, *Many-Body Quantum Theory in Condensed Matter Physics. An Introduction* (Oxford University Press, Oxford, 2004), p. 464
25. A.F. Kemper, M.M. Korshunov, T.P. Devereaux, J.N. Fry, H.-P. Cheng, P.J. Hirschfeld, Phys. Rev. B **83**, 184516 (2011)
26. S. Maiti, J. Knolle, I. Eremin, A.V. Chubukov, Phys. Rev. B **84**, 144524 (2011)